Content

S1 Sea Salt Source functions

In order to combine, compare and integrate the functions introduced below some general assumptions and transformations are necessary that are described in (Eq. S1), (Eq. S2), and (Eq. S3). According to Lewis and Schwatz (2004) we assume

$$r_{80} = 2 \cdot r_{dry} = D_{dry} \tag{S1}$$

Following the above relation and basic calculus we get

$$\frac{dF}{dr_{80}} = \frac{dF}{dD_{dry}} \tag{S2}$$

$$\frac{dF}{dD_{dry}} = \frac{d\ln D_{dry}}{dD_{dry}} \cdot \frac{dF}{d\ln D_{dry}} = \frac{1}{D_{dry}} \cdot \frac{dF}{d\ln D_{dry}} = \frac{1}{\ln 10 \cdot D_{dry}} \cdot \frac{dF}{d\log_{10} D_{dry}} \tag{S3}$$

S1.1 MO86

Monahan and colleagues (Monahan & Muircheartaigh 1980; Monahan et al. 1982) described the generation of sea salt particles from bursting bubbles. They fitted a power law shaped whitecap coverage function to the wind speed in 10 m height (Eq. S4) (Monahan & Muircheartaigh 1980). A sea salt particle number flux distribution was estimated for 100% whitecap coverage and multiplied by W (Monahan et al. 1986).

$$W = 3.84 \cdot 10^{-6} \cdot u_{10}^{3.41} \tag{S4}$$

$$\frac{dF_{MO86}}{dr_{80}} = W \cdot 3.576 \cdot 10^{5} \cdot r_{80}^{-3} \cdot 10^{1.19 \cdot e^{-B^2}}$$

$$= 1.373 \cdot u_{10}^{3.41} \cdot r_{80}^{-3} \cdot 10^{1.19 \cdot e^{-B^2}} \tag{S5}$$

$$B = \frac{0.380 - \log_{10}(r_{80})}{0.650}$$

The parameterization is valid on the size range 0.8 µm < r_{80} < 20 µm.

S1.2 GO03

Gong (2003) updated Monahan et al. (1986) for smaller size ranges.

$$\frac{dF_{GO03}}{dr_{80}} = W \cdot 3.576 \cdot 10^{5} \cdot r_{80}^{-A} \cdot \left(1 + 0.057 \cdot r_{80}^{3.45}\right) \cdot 10^{1.607 \cdot e^{-B^2}}$$

$$= 1.373 \cdot u_{10}^{3.41} \cdot r_{80}^{-A} \cdot \left(1 + 0.057 \cdot r_{80}^{3.45}\right) \cdot 10^{1.607 \cdot e^{-B^2}} \quad \text{(S6)}$$

$$A = 4.7 \cdot (1 + \theta \cdot \mathrm{r}_{80})^{-0.017 \cdot \mathrm{r}_{80}^{-1.44}}, \quad B = \frac{0.433 - \log_{10}(r_{80})}{0.433}$$

where θ is an adjustable parameter without any unit that is set to 30. The parameterization is valid on the size range 0.07 µm < r_{80} < 20 µm.

S1.3 SM93

Smith et al. (1993) fitted log normal distributions to coarse sea salt particle measurements.

$$\frac{dF_{SM93}}{dr_{80}} = \sum_{k=1}^{2} A_k(u_{10}) \cdot \exp\left\{-f_k \left(\ln\left(\frac{r_{80}}{r_{0k}}\right)\right)^2\right\} \quad \text{(S7)}$$

$$\log_{10}(A_1) = 0.0676 \cdot u_{10} + 2.43$$

$$\log_{10}(A_2) = 0.959 \cdot u_{10}^{0.5} - 1.476$$

$$r_{01} = 2.1\ \mu m; \qquad r_{02} = 9.2\ \mu m$$

$$f_1 = 3.1; \qquad f_2 = 3.3$$

Spada et al. (2013) considers the parameterization to be valid on the size range of 5 µm < r_{80} < 30 µm.

S1.4 MA03

Mårtensson et al. (2003) performed laboratory studies on SST and SAL dependence of sea salt emissions. They derived a SST dependent particle number flux parameterization. The whitecap coverage parameterization from Monahan and Muircheartaigh (1980) was employed (Eq. S4).

$$\frac{dF_{MA03}}{dD_{dry}} = W * (A * SST + B) \quad \text{(S8)}$$

$$A = c_4 \cdot D_{dry}^4 + c_3 \cdot D_{dry}^3 + c_2 \cdot D_{dry}^2 + c_1 \cdot D_{dry} + c_0$$

$$B = d_4 \cdot D_{dry}^4 + d_3 \cdot D_{dry}^3 + d_2 \cdot D_{dry}^2 + d_1 \cdot D_{dry} + d_0$$

where c_i and d_i are constants given in Table S1. They have to be chosen according to D_{dry}. This parameterization is valid on the size range of 0.02 µm < D_{dry} < 2.8 µm and on the temperature range of 271 K < SST < 298 K.

Table S1: Constants for (Eq. S8). Values are taken from Martensson et al. (2003)[Table 1] but given with more significant digits (personal communication, Martensson, 2015).

D_{dry} interval [µm]	c_4	c_3	c_2	c_1	c_0
0.020 - 0.145	-2.5761655e+35	+5.9324436e+28	-2.8671743e+21	-3.0029837e+13	-2.8808135e+6
0.145 - 0.419	-2.4522893e+33	+2.4035441e+27	-8.1478341e+20	+1.1828503e+14	-6.7429939e+6
0.419 - 2.800	+1.0851561e+29	-9.8414340e+23	+3.1323593e+18	-4.1645326e+12	+2.1806374e+6
D_{dry} interval [µm]	**d_4**	**d_3**	**d_2**	**d_1**	**d_0**
0.020 - 0.145	+7.1884656E+37	-1.6156647E+31	+6.7913299E+23	+1.8289469E+16	+7.6092681E+8
0.145 - 0.419	+7.3683150E+35	-7.3102149E+29	+2.5283404E+23	-3.7872729E+16	+2.2794005E+9
0.419 - 2.800	-2.8594762E+31	+2.6012137E+26	-8.2974644E+20	+1.1046678E+15	-5.8003880E+8

S1.5 SP13

Spada et al. (2013) compared several source functions and combinations of them on a global scale: They considered an extension of GO03 by SST (Jaegle et al., 2013) and MA03/MO86/SM93 (Martensson et al., 2013; Monahan et al., 1986; Smith et al., 1993). The latter one is used in this study and abbreviated as SP13.

$$\frac{dF_{SP13}}{dD_{dry}} = \begin{cases} \frac{dF_{MA03}}{dD_{dry}} & D_{dry} \leq 2.8\,\mu m \\ \frac{dF_{MO86}}{dD_{dry}} & D_{dry} > 2.8\,\mu m \ \wedge u_{10} < 9\frac{m}{s} \\ \max\left(\frac{dF_{MO86}}{dD_{dry}}, \frac{dF_{SM93}}{dD_{dry}}\right) & D_{dry} > 2.8\,\mu m \ \wedge u_{10} \geq 9\frac{m}{s} \end{cases} \quad \text{(S9)}$$

Because of (Eq. S2), we do not need to rewrite (Eq. S5) and (Eq. S7). SP13 is valid on the size range 0.02 µm < D_{dry} < 30 µm.

S1.6 OV14

Recently, Ovadnevaite et al. (2014) published a new parameterization depending on wave state, wind speed and sea water viscosity whereby the viscosity depends on SAL and SST.

$$\frac{dF_{OV14}}{d\log_{10} D_{dry}} = \sum_{i=1}^{5} \frac{F_i(Re_{H_W})}{\sqrt{2\,\pi}\cdot\log_{10}(\sigma_i)} \cdot \exp\left\{-\frac{1}{2}\cdot\left(\frac{\log_{10}\left(\frac{D_{dry}}{\mathrm{GMD}_i}\right)}{\log_{10}(\sigma_i)}\right)\right\} \quad \text{(S10)}$$

$$Re_{H_W} = \frac{u_* \cdot H_S}{\nu_W} = \frac{\sqrt{C_D}\cdot u_{10}\cdot H_S}{\nu_W} \quad \text{(S11)}$$

The factors GMD_i and σ and the functions $F_i(Re_{HW})$ are given in Table S2. The kinetic viscosity ν_W is calculated according to equations (Eq. 22) and (Eq. 8) in Sharqawy et al. (2010). When C_D is not taken from a model (outside the North Sea), it is calculated according to Wu (1982) as given in equation (Eq. S12). The source function is valid for a diameter size range of 0.015 µm < D_{dry} < 6 µm. For integrating one needs to rewrite it with (Eq. S3) and to get a derivative to dD_{dry}.

Table S2: Values for (Eq. S10) from Ovadnevaite et al. (2014) but given with more significant digits (personal communication, Ovadnevaite, 2015). When one wants to reconstruct figure 4 in Ovadnevaite et al. (2014) with these values, one gets slight deviations due to rounding.

Mode (i)	$\mathrm{GMD}_i\ [\mu m]$	$\sigma_i\ [\mu m]$	$F_i(Re_{H_W})$
1	0.018	1.37	$104.51\cdot\left(Re_{H_W}-10^5\right)^{0.556}$
2	0.041	1.50	$0.044\cdot\left(Re_{H_W}-10^5\right)^{1.08}$
3	0.090	1.42	$149.64\cdot\left(Re_{H_W}-10^5\right)^{0.545}$
4	0.230	1.53	$2.96\cdot\left(Re_{H_W}-10^5\right)^{0.79}$
5	0.830	1.85	$0.52\cdot\left(Re_{H_W}-10^5\right)^{0.87}$

The drag coefficient C_D is calculated according to Wu (1982) for regions where no coastDatII WAM data were available

$$C_D = \begin{cases} 1.2875\cdot 10^{-3}, & \text{for } u_{10} < 7.5\frac{m}{s} \\ \left(0.8 + 0.065\frac{m}{s}\cdot u_{10}\right)\cdot 10^{-3}, & \text{for } u_{10} \geq 7.5\frac{m}{s} \end{cases} \quad \text{(S12)}$$

The friction velocity u_* is calculated from C_D by

$$u_* = u_{10} \cdot \sqrt{C_D} \tag{S13}$$

S2 Surf Zone Treatment

The surf zone is implemented in accordance with Kelly et al. (2010) by setting the whitecap coverage to 1 within it. For each grid cell, the fraction of open ocean and surf zone is calculated in accordance with Neumann et al. (2015) and denoted as OPEN and SURF, respectively. In (Eq. S5), (Eq. S6), and (Eq. S8) the W is replaced by (Eq. S14)

$$(W \cdot \mathrm{OPEN} + \mathrm{SURF}) \cdot \frac{1}{W} \tag{S14}$$

Exemplary, applying this to GO03 (Eq. S6) leads to (Eq. S15).

$$\frac{dF_{GO03,net}}{dr_{80}} = (W \cdot \mathrm{OPEN} + \mathrm{SURF}) \cdot \frac{1}{W} \cdot \frac{dF_{GO03}}{dr_{80}} \tag{S15}$$
$$= (W \cdot \mathrm{OPEN} + \mathrm{SURF}) \cdot 3.576 \cdot 10^5 \cdot r_{80}^{-A} \cdot \left(1 + 0.057 \cdot r_{80}^{3.45}\right) \cdot 10^{1.607 \cdot e^{-B^2}}$$

S3 Salinity Dependence

For this study, the GO03 and SP13 parameterizations were enhanced by a salinity dependence. Figure S1 shows the dependence for three exemplary salinities. We assumed that the sea salt emission parameterizations were derived for a sea surface salinity of 35‰.

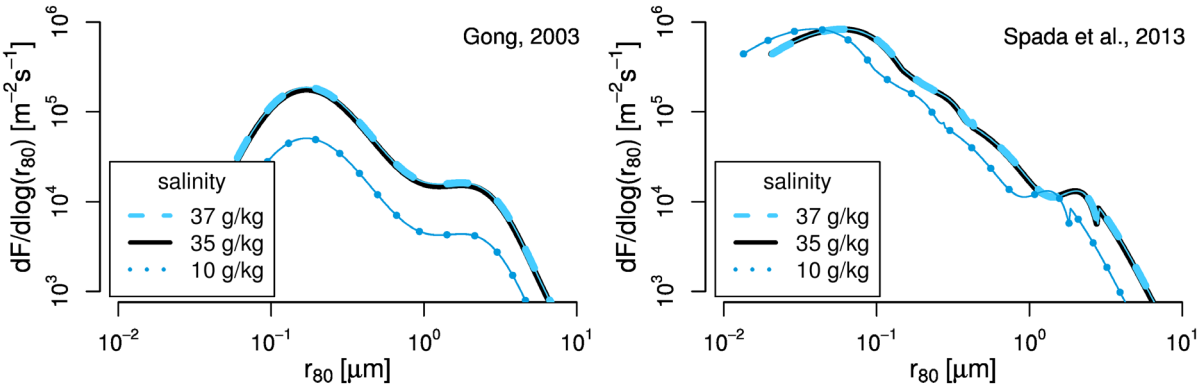

Figure S1: Salinity dependence of the GO03 (left) and SP13 (right) parameterizations as implemented in this study. Parameters are choosen according to Fig. 2 in the main manuscript: u_{10} = 8 m/s, SST = 283 K, C_D = 2.15e-3, H_S = 1.23 m, and ν_W = 1.34e-6 m^2/s.

S3.1 GO03

The sea salt emissions number, surface area and mass (or volume) emissions are all scaled by the salinity SAL:

$$\frac{dF_{\mathrm{GO03,net}}}{dr_{80}} = \frac{\mathrm{SAL}}{35‰} \cdot (W \cdot \mathrm{OPEN} + \mathrm{SURF}) \cdot \frac{1}{W} \cdot \frac{dF_{\mathrm{GO03}}}{dr_{80}} \tag{S16}$$

Because GO03 sea salt emissions are calculated within CMAQ, one solution for implementing the salinity dependence was to modify CMAQ code. Because OPEN and SURF are read in externally from the OCEANfile (see CMAQ documentation), one can rewrite (Eq. S16) to (Eq. S17) and scale OCEAN and SURF with SAL/35‰. Thus, no modifications in CMAQ are necessary.

$$\frac{dF_{\mathrm{GO03,net}}}{dr_{80}} = \left(W \cdot \frac{\mathrm{SAL}}{35‰} \cdot \mathrm{OPEN} + \frac{\mathrm{SAL}}{35‰} \cdot \mathrm{SURF}\right) \cdot \frac{1}{W} \cdot \frac{dF_{\mathrm{GO03}}}{dr_{80}} \quad \text{(S17)}$$

This approach was chosen in this study. OPEN and SURF are considered to be constant in time. This approach does not allow including annual or diurnal variations of the salinity dependence.

S3.2 SP13

We assume that (a) inorganic ions are homogeneously distributed in the water column (no enrichment at the sea surface or in deeper water layers) and that (b) the water droplet generation process is not affected by variable salinity. Then sea surface salinity and gross dry sea salt mass emissions are proportional to each other because the droplet emission distribution does not change but the sea salt concentration within them does change. Further we assume that we can apply the same relation to net sea salt emissions. This assumption is not completely correct. Thus, in a region with 17.5‰ salinity, the dry sea salt mass emissions should be half as high compared with the emissions in a region with 35‰ salinity. The sea salt number emissions should remain unchanged but the dry mass of sea salt per individual sea salt particle $m_{\mathrm{dry,SAL}}$ should vary as described:

$$m_{\mathrm{dry,SAL}} = \frac{\mathrm{SAL}}{35‰} \cdot m_{\mathrm{dry,35‰}} \quad \text{(S18)}$$

Dry sea salt particle volume and dry sea salt particle mass are proportional to each other. Therefore, for the volume (V), surface area (A), and diameter (D) of individual sea salt particles follows:

$$V_{\mathrm{dry,SAL}} = \frac{\mathrm{SAL}}{35‰} \cdot V_{\mathrm{dry,35‰}} \quad \text{(S19)}$$

$$A_{\mathrm{dry,SAL}} = \left(\frac{\mathrm{SAL}}{35‰}\right)^{2/3} \cdot A_{\mathrm{dry,35‰}} \quad \text{(S20)}$$

$$D_{\mathrm{dry,SAL}} = \left(\frac{\mathrm{SAL}}{35‰}\right)^{1/3} \cdot D_{\mathrm{dry,35‰}} \quad \text{(S21)}$$

If (Eq. S21) is applied to the particle emission size distribution in (Eq. S9) then the particle diameter needs to be scaled accordingly yielding a shift of the distribution by $\left(\sqrt[3]{\mathrm{SAL}/35‰} - 1\right) \cdot D_{dry}$ to the right. If SAL < 35‰ then the shift is performed to the left (Figure S1).

S4 Integrating SP13 and OV14

The two sea salt source functions (Eq. S10) and (Eq. S24 + S9) were integrated as described in section 3.2.3 of the manuscript, in Table S3, and in Figure 2. Equation (Eq. S9) was enhanced to depend on SAL as described in section S3.

Table S3: Overview of the integration of SP13 and OV14. This table should be considered in combination with Figure 3 in the main manuscript. $D_{dry,min,SAL}$ and $D_{dry,max,SAL}$ denote the minimum and maximum diameters, respectively, for those the SP13 parameterization is defined (see section S3.2). $D_{dry,Aa}$ and $D_{dry,ac}$ are the integration boundaries between the Aitken and accumulation mode and between the accumulation and coarse mode, respectively.

Size mode	SP13	OV14
Aitken	Whole function integrated from $D_{dry,min,SAL}$* to $D_{dry,Aa}$ (= 0.1 µm)	Modes 1 and 2 integrated from 0.015 µm to 6 µm
accumulation	Whole function integrated from $D_{dry,Aa}$ µm to $D_{dry,ac}$**	Modes 3 and 4 integrated from 0.015 µm to 6 µm
coarse	Whole function integrated from $D_{dry,ac}$** µm to $D_{dry,max,SAL}$*	Mode 5 integrated from 0.015 µm to 6 µm

* see section S4.1 for details; ** see Table S4 for appropriate values

The water content of wet sea salt – compared to dry – was calculate in accordance with Lewis and Schwartz (2004)[p.54] (or Lewis and Schwartz (2006) for exactly this formulation):

$$\frac{D_{\mathrm{RH}}}{D_{80}} = 0.54 \cdot \left(\frac{2-\mathrm{RH}}{1-\mathrm{RH}}\right)^{\frac{1}{3}} \qquad \text{(S22)}$$

S4.1 Integration boundaries for SP13

We decided that the integration boundary between accumulation and coarse mode ($D_{dry,ac}$) for integrating SP13 dry sea salt emissions should equal the intersection between GO03 accumulation- and coarse-mode distributions as defined in CMAQ. In CMAQ, the distributions are dependent on the relative humidity (RH). Therefore, the intersection diameter for each RH was calculated and converted to dry diameter (Table S4). The resulting dry diameter still depends on RH which is an artifact. However, we kept this dependence in order to be consistent with GO03.

Table S4: RH dependent integration boundary between accumulation and coarse mode as dry diameter $D_{dry,ac}$ for integrating the SP13 parameterization.

RH [%]	$D_{dry,ac}$ [µm]	RH [%]	$D_{dry,ac}$ [µm]
45	1.276076	…	…
50	1.324269	80	1.498309
55	1.347672	85	1.490230
60	1.388263	90	1.514228
65	1.415549	93	1.550082
70	1.453910	95	1.578587
75	1.479312	97	1.577349
…	…	99	1.361808

Including SAL dependence into the integration of SP13 is not straightforward. Therefore, it is described in detail below. We define a function f_{SP}

$$f_{sp}(D_{\mathrm{dry}}) = \frac{dF_{\mathrm{SP13}}}{dD_{\mathrm{dry}}} \qquad \text{(S23)}$$

in order to express the SAL dependence mathematically by

$$\frac{dF_{\mathrm{SP13,SAL}}}{dD_{\mathrm{dry}}} = f_{sp,\mathrm{SAL}}(D_{\mathrm{dry}}) = f_{sp}\left(D_{dry} \cdot \left(\frac{35‰}{\mathrm{SAL}}\right)^{1/3}\right) \quad \text{(S24)}$$

The SAL dependent source function as defined by (Eq. S24) is not valid on the same interval as (Eq. S9) anymore; that was

$$D_{\mathrm{dry,min}} = 0.02\ \mu m < D_{\mathrm{dry}} < 30\ \mu m = D_{\mathrm{dry,max}}$$

But rather it is valid on the interval

$$D_{\mathrm{dry,min,SAL}} = 0.02\ \mu m \cdot \left(\frac{\mathrm{SAL}}{35‰}\right)^{1/3} < D_{\mathrm{dry}} < 30\ \mu m \cdot \left(\frac{\mathrm{SAL}}{35‰}\right)^{1/3} = D_{\mathrm{dry,max,SAL}}$$

Further, we define that the boundaries between Aitken and accumulation mode (D_{Aa}) and between accumulation and coarse mode (D_{ac}) remain unaffected. $D_{\mathrm{dry,ac}}(\mathrm{RH})$ is defined in Table S4.

$$D_{\mathrm{dry,Aa}} = 0.1\ \mu m$$

$$D_{\mathrm{dry,ac}} = D_{\mathrm{dry,ac}}(\mathrm{RH})$$

The dry sea salt number, surface area, and volume emissions are integrated based on these definitions and assumptions (Table S5). Dry mass emissions are calculated from the volume emissions by multiplication with $\rho_{sea\ salt}$ which is considered to be 2.2 g/cm^3.

Table S5: Integrals for calculating SAL dependent SP13 sea salt emissions.

	Number Emissions	**Surface area Emissions**	**Volume Emissions**
Aitken	$\int_{D_{min}\cdot\sqrt[3]{\frac{S}{35‰}}}^{D_{Aa}} f_{SP}\left(\frac{D}{\sqrt[3]{\frac{S}{35‰}}}\right) dD$	$\int_{D_{min}\cdot\sqrt[3]{\frac{S}{35‰}}}^{D_{Aa}} \pi D^2 f_{SP}\left(\frac{D}{\sqrt[3]{\frac{S}{35‰}}}\right) dD$	$\int_{D_{min}\cdot\sqrt[3]{\frac{S}{35‰}}}^{D_{Aa}} \frac{\pi}{6} D^3 f_{SP}\left(\frac{D}{\sqrt[3]{\frac{S}{35‰}}}\right) dD$
acc.	$\int_{D_{Aa}}^{D_{ac}} f_{SP}\left(\frac{D}{\sqrt[3]{\frac{S}{35‰}}}\right) dD$	$\int_{D_{Aa}}^{D_{ac}} \pi D^2 f_{SP}\left(\frac{D}{\sqrt[3]{\frac{S}{35‰}}}\right) dD$	$\int_{D_{Aa}}^{D_{ac}} \frac{\pi}{6} D^3 f_{SP}\left(\frac{D}{\sqrt[3]{\frac{S}{35‰}}}\right) dD$
coarse	$\int_{D_{ac}}^{D_{max}\cdot\sqrt[3]{\frac{S}{35‰}}} f_{SP}\left(\frac{D}{\sqrt[3]{\frac{S}{35‰}}}\right) dD$	$\int_{D_{ac}}^{D_{max}\cdot\sqrt[3]{\frac{S}{35‰}}} \pi D^2 f_{SP}\left(\frac{D}{\sqrt[3]{\frac{S}{35‰}}}\right) dD$	$\int_{D_{ac}}^{D_{max}\cdot\sqrt[3]{\frac{S}{35‰}}} \frac{\pi}{6} D^3 f_{SP}\left(\frac{D}{\sqrt[3]{\frac{S}{35‰}}}\right) dD$

S5 Input Data

Figure S2 shows the regions that are covered by different sets of input data. The COSMO-CLM meteorological data set covers the whole study region and is not marked in the map. ERA-Interim wave and ocean data were used outside of the blue and orange colored regions except for SAL. SAL was set to 35‰ in the Atlantic Ocean, 37‰ in the Mediterranean Sea, and 18‰ in the Black Sea. Table S6 shows the source and resolution of the input data that were used for calculation sea salt emissions for the five sea regions – North Sea, Baltic Sea, Atlantic Ocean, Mediterranean Sea, and Black Sea.

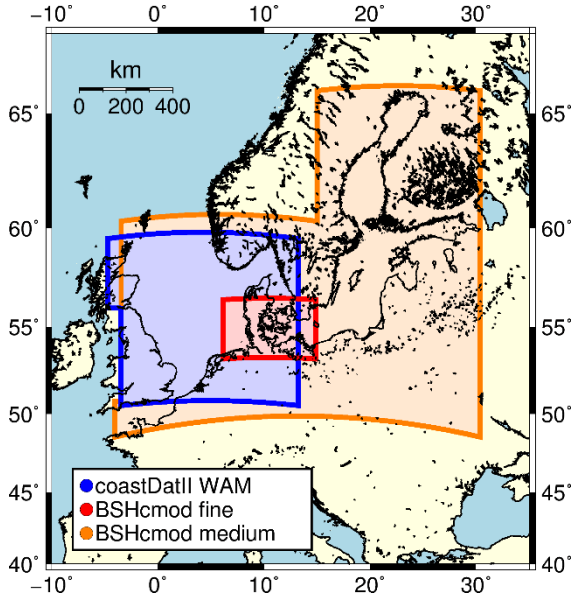

Figure S2: Map showing the locations corresponding to the input data from each source. **Wave data:** In the blue region, wave data from coastDatII were used. Outside this region, the significant wave height data were acquired from ERA-Interim and the friction velocity data were calculated based on meteorological input data. **SST and SAL data:** In the orange and red regions, SST and SAL data were acquired from BSHcmod with medium and fine grid resolutions, respectively. Outside the orange region, the SST data were acquired from ERA-Interim and the SAL was set to a fixed value (see text). **Meteorological data:** The same meteorological data were used for the entire map region.

Table S6: Overview of the input data used for calculating sea salt emissions

Parameter	**Resolution**	**Region**	**Model [Database]**	**Reference**
Meteorology	0.22° x 0.22° lon x lat, rotated	Whole model region	CCLM v4.8 [coastDatII]	Geyer & Rockel (2013), Geyer (2014)
Waves (H_S, C_D)	0.075° x 0.05° lon x lat	North Sea (southward of 59,2° N and eastward of 4.75° W)	WAM 4.5.3 [coastDatII]	Groll et al. (2014)
Waves (H_S)	1° x 1°	Atlantic Ocean, Baltic Sea, Mediterranean Sea, Black Sea	WAM [ERA-Interim]	Dee et al. (2011)
Waves (u_*)	see Meteorology	Atlantic Ocean, Baltic Sea, Mediterranean Sea, Black Sea	derived from u_{10} [coastDatII]	Wu (1982)
SST, SAL	5’ x 3’ lon x lat	North and Baltic Sea	BSHcmod4, coarse grid	Dick et al. (2001), BSH*
SST, SAL	50’’ x 30’’ lon x lat	German waters in North and Baltic Sea	BSHcmod4, fine grid	Dick et al. (2001), BSH*
SST	1° x 1°	Atlantic Ocean, Mediterranean Sea, Black Sea	ERA input only [ERA-Interim, NCEP]	
SAL	/	Atlantic Ocean, Mediterranean Sea, Black Sea	Atlantic: 35‰, Med. Sea: 37‰, Black Sea: 18‰,	

* http://www.bsh.de/en/Marine_data/Forecasts/Prediction_models/index.jsp

S6 Modifications in CMAQ

S6.1 Changes in the CMAQ Code

The modules AERO_EMIS.F (minor changes) and SSEMIS.F were modified. All other modules were kept unchanged. The modified source code files are attached in the supplement. Modifications in the modules and subroutines/functions are documented in the beginning of each one by "[DATE] Neumann: ..." and indicated in the code by "NEUMANND". There are four types of comment indication modifications:

1. new variables

```
! NEW VARIABLES BY NEUMANND
[VARIABLE DEFINITION]
```

2. long new code passages

```
! START NEUMANND
[CODE]
! END NEUMANND
```

3. individual new code lines

```
! NEW NEUMANND: [DESCRIPTION]
[CODE] ! NEW
```

4. individual modified code lines

```
! MODIFIED NEUMANND: [DESCRIPTION]
[CODE] !
```

S6.2 Changes in the Namelist files

If Aitken mode sea salt emissions are read in, they should be displayed in the output files. For this purpose the aerosol namelist file (AE_cb05tucl_ae5_aq.nml) needs to be modified. In the line starting with “ANAI”, the columns DDEP, WDEP and CONC have be set to “Yes”. Alternatively, one can replace the line

```
'ANAI:23.0:ANAI:1.0:VMASSI:1.0:NA_AITKEN:1.0:::NA_AITKEN:Yes:::',
```

by the line

```
'ANAI:23.0:ANAI:1.0:VMASSI:1.0:NA_AITKEN:1.0:::NA_AITKEN:Yes:Yes:Yes:Y
es',
```

S6.3 Additions in the CMAQ Run Script

Two new environment variables need to be set in the CMAQ run script in order to read in sea salt emissions externally. Below, a code example is given:

```
#> read sea-salt emissions from external file [ N|F ]
setenv CTM_READSSEMIS Y

#> Sea Salt emissions
set SS_FILE = SSEMIS.${STDATE}  # example file name
set SS_DIR  = /example/ssemis    # example directory name

#> file containing the sea-salt emissions
setenv SSEMIS_1 ${SS_DIR}/${SS_FILE}
```

S7 Setup of CMAQ runs

The 24 x 24 km^2 and 72 x72 km^2 grids are denoted as CD24 and CD72 grids and defined in the attached GRIDDESC file.

Six OCEAN files are attached – three for each grid. The identifier “sf050m” indicates that a surf zone of 50 m width is assumed. The identifier “_sal” indicates that the OPEN and SURF variables are scaled by the salinity as described in section S3.1. The identifier “_noSalt” indicates that OPEN and SURF are set to 0 (zero) so that no sea salt is emitted. The identifier “_GIS_ubound” indicates that the coastline data were extracted via ArcGIS in accordance with Neumann et al. (2015) and that the SURF variable has an upper bound (Neumann et al., 2015). Table S7 shows which OCEAN file was used for each emission case.

Table S7: Usage of the three OCEAN files in the four sea salt emission cases. The asterix replaces CD24 and CD72.

Case	OCEAN file
zero	OCEAN_*_noSalt_GIS.nc
GO03	OCEAN_*_sf050m_GIS_ubound_sal.nc
SP13	OCEAN_*_sf050m_GIS_ubound.nc
OV14	OCEAN_*_sf000m_GIS_ubound.nc

S8 Emissions

The Figures S3 to S5 show sea salt mass, surface area, and number emissions, respectively, at one location in the German Bight. Figure S6 shows the GMD of the emissions at the same locations. In each figure, Aitken-, accumulation- and coarse-mode emissions are plotted (top to bottom). The plots show winter (left) and summer emissions (right).

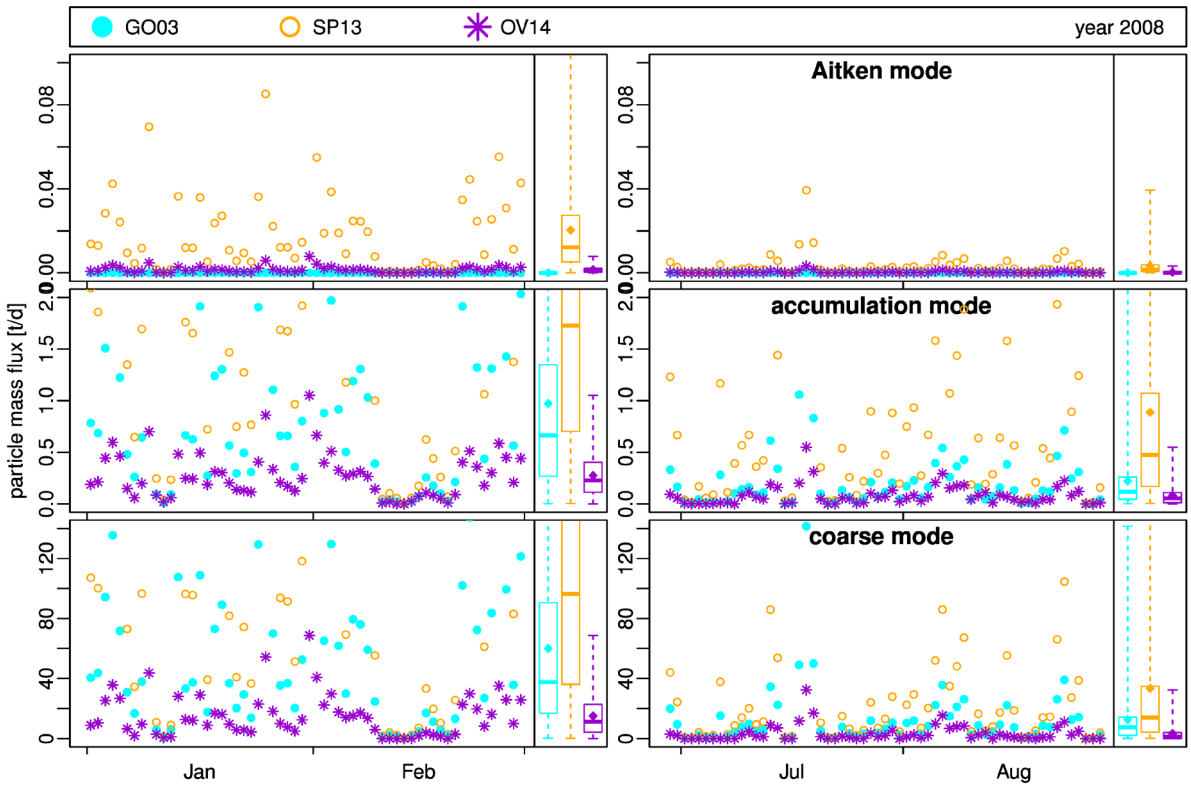

Figure S3: Sea salt mass emissions [t/d] into the Aitken, accumulation, and coarse modes (top top bottom) at one location in the German Bight in winter (left) and summer (right) 2008.

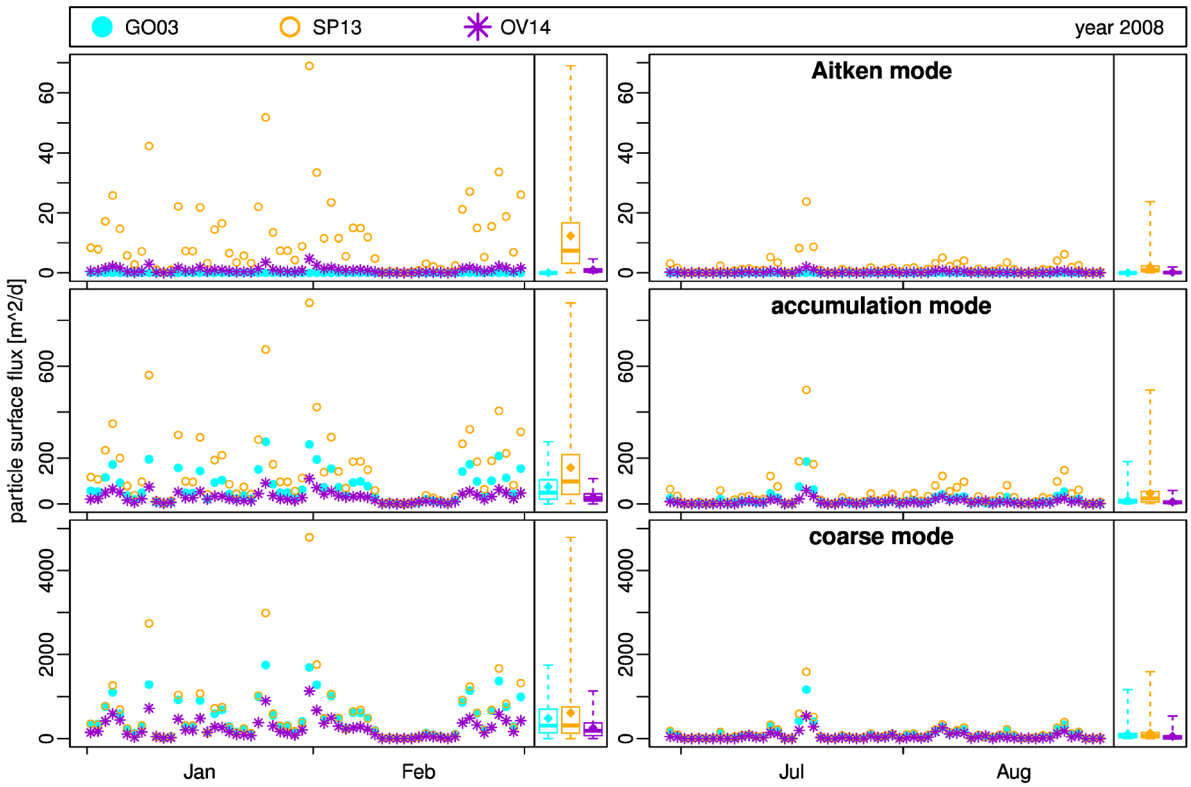

Figure S4: Similar to Figure S3 but showing sea salt particle surface area emissions [m^2/d].

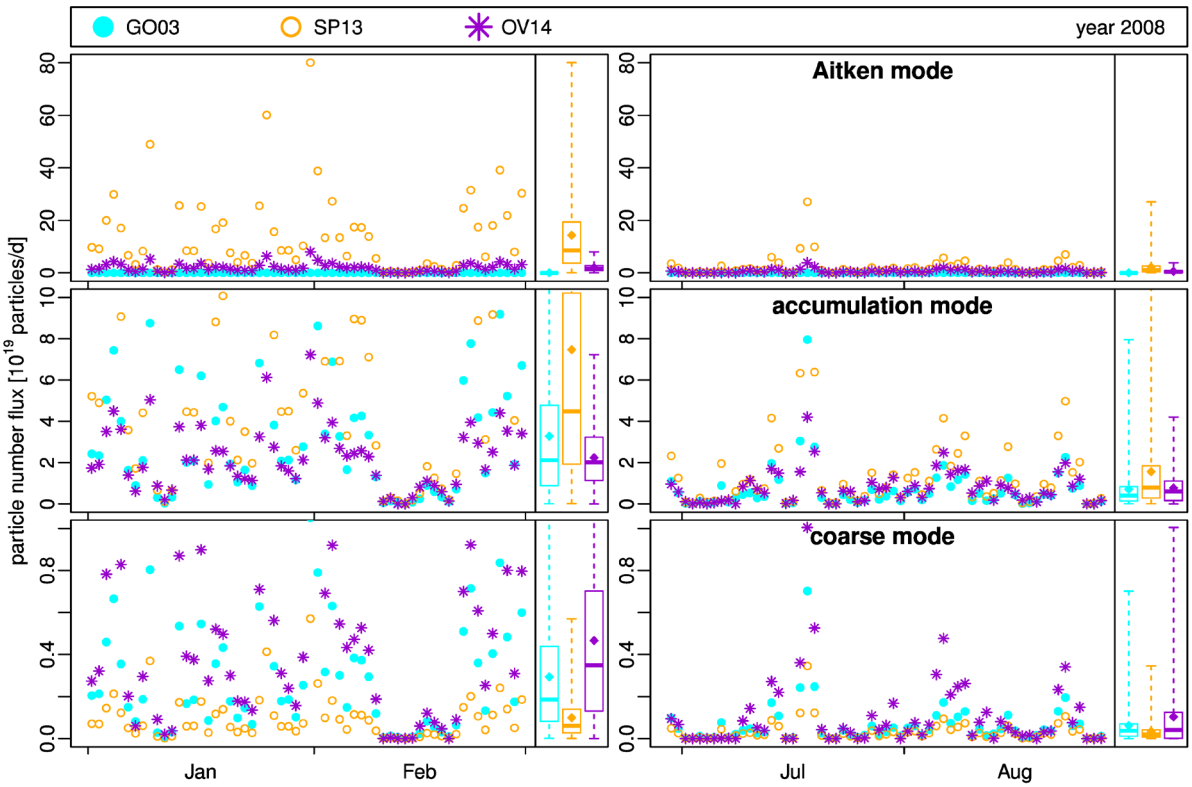

Figure S5: Similar to Figure S3 but showing sea salt particle number emissions [10^{19} particles/d].

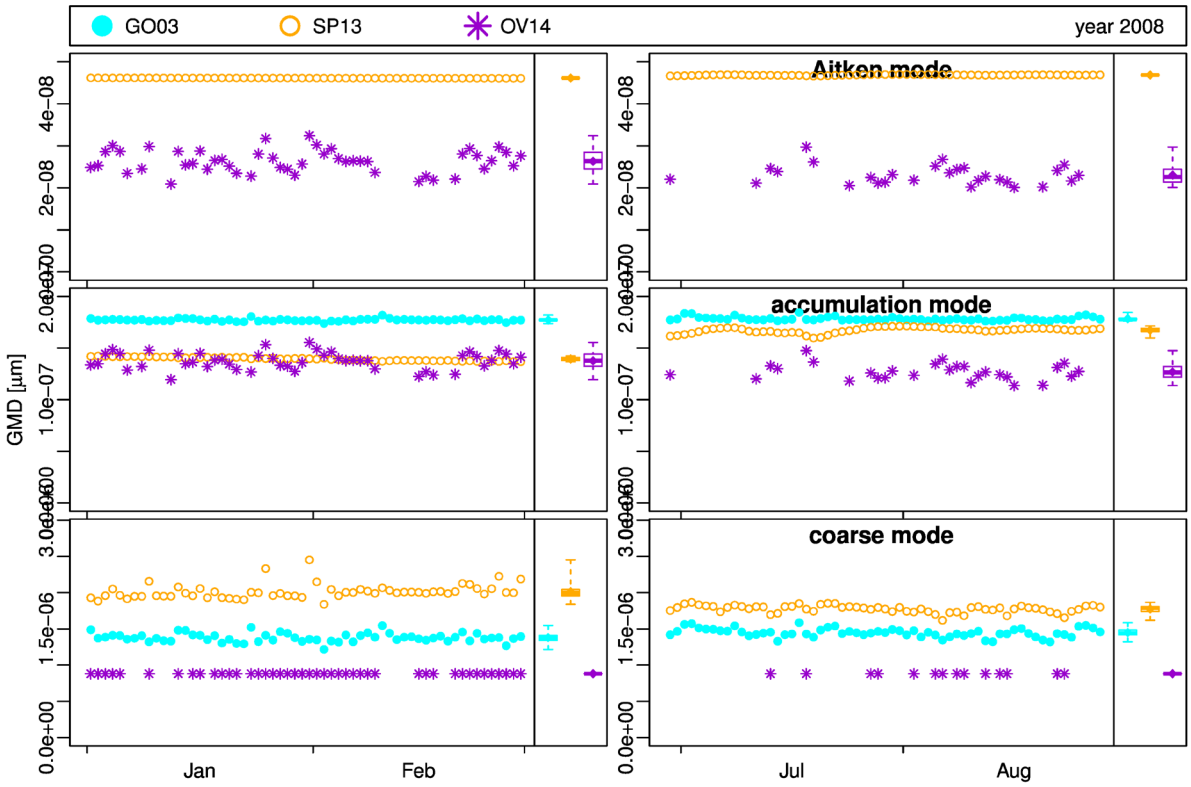

Figure S6: Similar to Figure S3 but showing the geometric mean diameter (GMD) of the emitted sea salt particle Aitken, accumulation and coarse mode distributions (top to bottom). Log-normal distributed modes are assumed in order to calculate GMD and σ (Binkowski and Roselle, 2003). As Figure 2 (Paper) shows, this assumption is not justified. However, log-normal shaped emissions and concentrations are assumed in CMAQ.